PCCP

RSC Publishing

PAPER

Interaction of TiO^+ with water: infrared photodissociation spectroscopy and density functional calculations†

Cite this: *Phys. Chem. Chem. Phys.*, 2013, **15**, 17126

Hong-Guang Xu,[a] Xiao-Na Li,*[b] Xiang-Yu Kong,[a] Sheng-Gui He[b] and Wei-Jun Zheng*[a]

Received 5th July 2013,
Accepted 13th August 2013

DOI: 10.1039/c3cp52823e

www.rsc.org/pccp

We investigated the interaction of TiO^+ with water by conducting infrared photodissociation spectroscopy and density functional theory calculations on $TiO(H_2O)Ar^+$ and $TiO(H_2O)_{5-7}^+$ clusters. The studies show that $TiO(H_2O)Ar^+$ has two isomers, $Ti(OH)_2Ar^+$ and (H_2O)–$TiOAr^+$, coexisting in our experiments. The structure of $TiO(H_2O)_5^+$ is characterized by attaching four water molecules to a $Ti(OH)_2^+$ core with their O atoms interacting with the Ti atom directly. With the increasing number of water molecules, the additional water molecules start to form hydrogen bonds with the inner shell water molecules and the OH groups of $Ti(OH)_2^+$ instead of coordinating directly with the Ti atom. Therefore, the structures of $TiO(H_2O)_6^+$ and $TiO(H_2O)_7^+$ clusters are evolved from that of $TiO(H_2O)_5^+$ by adding the sixth and seventh water molecules to the second solvent-shell. Our results demonstrate that a $Ti(OH)_2^+$ type of product is dominant when TiO^+ interacts with water, especially when more water molecules are involved.

I. Introduction

It is very important to understand the interactions between transition-metal oxides (TMOs) and water because they are strongly related with the applications of TMOs on catalysis and materials.[1–3] Therefore, extensive studies have been devoted to investigate the TMO–water interactions in the last few decades.[4,5] Johnson and Panas investigated water adsorption and hydrolysis on a number of TMOs and oxyhydroxides with density functional calculations.[6,7] Schwarz and co-workers studied the reactions of VO^+ ions[8] and $V_mO_n^+$ (m = 1–4, n = 1–10) ions[9] with water molecules by mass spectrometry and the interaction of FeO^+ with water by density functional calculations.[10] The reactions between vanadium oxide ions and water were also investigated by Ma *et al.*[11] and Li *et al.*[12] using fast flow reactor experiments and density functional calculations. Jarrold and co-workers investigated the reactions of water with tungsten oxides[13–15] and molybdenum oxides[16] using a high-pressure fast-flow reactor combined with a time-of-flight mass spectrometer. Zhou and co-workers conducted matrix isolation spectroscopic studies of water adsorption on platinum oxides,[17] tantalum oxides and niobium oxides.[18] Recently, Li *et al.*[19] investigated the interaction of Co_mO^- with H_2O using anion photoelectron spectroscopy and found that the dihydroxide anions, $Co_m(OH)_2(H_2O)_n^-$, are more stable than the hydrated metal-oxide anions, $Co_mO(H_2O)_{n+1}^-$.

TiO is an important molecule detected in the atmospheres of stars.[20] It is also a valuable precursor for synthesis of single-crystal nanowires of TiO_2 [21] which has applications in many areas, such as pigments, coating materials, and catalysts, especially in photocatalytic water splitting.[22–28] TiO^+ ions are an important form of Ti(III) in aqueous solution and can be readily oxidized into TiO^{2+}, oxotitanium(IV) ions.[29] The interactions of TiO and its cation with water were investigated previously by a number of researchers. Hydrated TiO particles with a modified Ti/O surface have been studied by Blazevska-Gilev *et al.*[30] Deng *et al.*[31] studied the mass distributions of $TiO(H_2O)_n^+$ clusters generated by laser induced plasma reactions using a triple quadrupole mass spectrometer and optimized the structures of small $TiO(H_2O)_n^+$ (n = 1–5) clusters with *ab initio* calculations. Fatmi *et al.*[29] investigated the TiO^{2+} ion in aqueous solution using quantum mechanical charge field molecular dynamics simulation. In these studies, the TiO^+ and TiO^{2+} ions were treated as intact ions without further reaction with water molecules. On the other hand, many studies show that metal oxides interacting with H_2O can form hydrated metal-oxides or undergo

[a] *State Key Laboratory of Molecular Reaction Dynamics, Institute of Chemistry, Chinese Academy of Sciences, Beijing 100190, China. E-mail: zhengwj@iccas.ac.cn*
[b] *State Key Laboratory for Structural Chemistry of Unstable and Stable Species, Institute of Chemistry, Chinese Academy of Sciences, Beijing 100190, China. E-mail: lxn@iccas.ac.cn*

† Electronic supplementary information (ESI) available: Optimized geometries of the typical low-lying isomers of the $TiO(H_2O)^+$ cluster (Fig. S1). Cartesian coordinates for stable isomers of $TiO(H_2O)_n^+$ clusters (Table S1). See DOI: 10.1039/c3cp52823e

hydrogen-transfer to form dihydroxides.[32–40] Therefore, it is extremely important to explore the possibility of dihydroxide formation in order to obtain a more complete picture regarding the interaction of TiO^+ with water.

In order to understand the interaction of TiO^+ with water, here we employ size-selected infrared photodissociation (IRPD) spectroscopy[41,42] in conjunction with density functional theory (DFT) calculations to probe the geometric structures of the $TiO(H_2O)Ar^+$ and $TiO(H_2O)_n^+$ (n = 5–7) clusters.

II. Experimental and theoretical methods

Experimental method

The experiments were conducted on a home-built apparatus equipped with a laser vaporization supersonic cluster source and a reflectron time-of-flight mass spectrometer (RTOF-MS), which has been described elsewhere.[43] Briefly, the $TiO(H_2O)_n^+$ cluster cations were generated in the laser vaporization source by laser ablation of a rotating and translating disk target (13 mm diameter, Ti 99.9%) with the second harmonic of a nanosecond Nd:YAG laser (Continuum Surelite II-10). The typical laser power used in this work is about 10 mJ per pulse. A mixture of argon gas and water vapor with ~4 atm backing pressure was allowed to expand through a pulsed valve (General Valve Series 9) into the source to provide water molecules and to cool the formed clusters. The generated cluster cations were mass- analyzed with the RTOF-MS. To further study the clusters of interest, a selection–deceleration–dissociation–reacceleration procedure[43] was employed in the IRPD experiments. The cluster ions were mass selected with a pulsed mass-gate at the first space focus point of the RTOF-MS, decelerated with a DC electric field, then dissociated with a tunable pulsed infrared laser. The fragment ions and parent ions were then reaccelerated toward the reflectron zone and reflected to the microchannel plate (MCP) detector. The output from the MCP detector was amplified using a broadband amplifier and recorded with a 200 MHz digital card. The digitalized data were collected in a laboratory computer with home-made software. The tunable infrared laser used is an optical parametric oscillator–amplifier (OPO–A) system (LaserVision, Inc.) employing KTP and KTA crystals pumped by a Nd:YAG laser (Continuum Surelite II-10, 1064 nm). The typical laser power is about 5–10 mJ per pulse in the range of 3200–3900 cm^{-1}. The wavelengths of the OPO–A laser were calibrated using a commercial monochromator (Beijing BeiGuang Century Instrument Co., Ltd, WDG30-Z). The photodissociation experiments were conducted with the infrared laser on and off alternatively shot by shot. The photodissociation mass spectra were obtained by subtracting the data taken with the infrared laser off from the data with the infrared laser on. The IRPD spectra were obtained by plotting the yields of fragment ions against the wavenumber of the infrared laser beam.

Theoretical method

The geometry optimization and the vibrational frequency calculations of $TiO(H_2O)Ar^+$ and $TiO(H_2O)_n^+$ clusters were conducted by using the Becke's three-parameter hybrid functional combined with Lee–Yang–Parr's gradient-corrected correlation functional (B3LYP)[44,45] as implemented in the Gaussian 09 program package.[46] The 6-311+G(d, p) basis set was used for the Ti, O, and H atoms. No imaginary frequency has been found, indicating that the structures correspond to the real local minima. The simulated theoretical infrared spectra were produced based on the scaled vibrational frequencies and the intensities from theoretical calculations and fitted with Lorentzian functions of a full width at half-maximum of 10 cm^{-1}. The vibrational frequencies from theoretical calculations were scaled with a scale factor of 0.96, which is recommended for the B3LYP method.[47] For comparison, we have also conducted the calculations of $TiO(H_2O)Ar^+$ and $TiO(H_2O)_n^+$ clusters with the second-order Møller–Plesset (MP2) method using the same basis set. An attempt at calculations with the CCSD(T) method is unsuccessful because it is computationally too expensive for vibrational frequency calculations of these clusters. It is found that the results of the B3LYP method are in slightly better agreement with the experiments than those of the MP2 method. Therefore, we mainly discuss the results from the B3LYP functional in this work.

III. Results and discussion

A typical mass spectrum of $TiO(H_2O)_n^+$ clusters produced in the experiment is shown in Fig. 1. The intensities of the mass peaks for the $TiO(H_2O)_n^+$ series exhibit a maximum at $TiO(H_2O)_5^+$, indicating that there might be some special characters in the structure of $TiO(H_2O)_5^+$.

The experimental IRPD spectrum of the $TiO(H_2O)Ar^+$ cluster and the simulated theoretical IR spectra of its low-lying isomers are displayed in Fig. 2. The experimental IRPD spectra of $TiO(H_2O)_n^+$ (n = 5–7) clusters as well as the simulated theoretical IR spectra of their low-lying isomers are shown in Fig. 3–5, respectively. The experimental IRPD spectrum of the $TiO(H_2O)Ar^+$ cluster was acquired by monitoring the loss of the Ar atom as a function of the wavenumber of the infrared laser, while those of

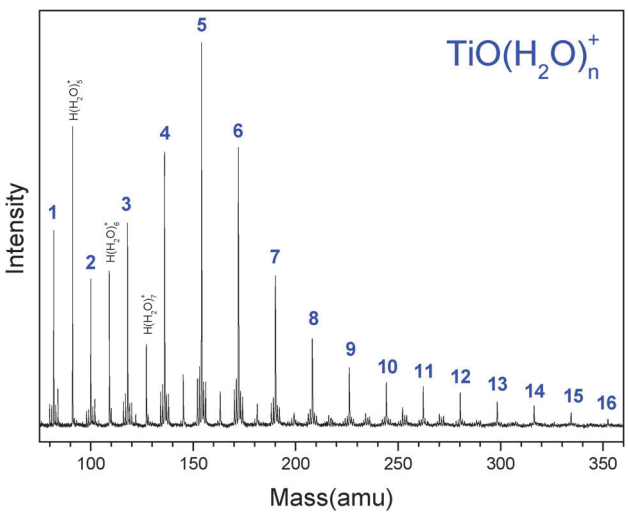

Fig. 1 Typical mass spectrum of $TiO(H_2O)_n^+$ clusters.

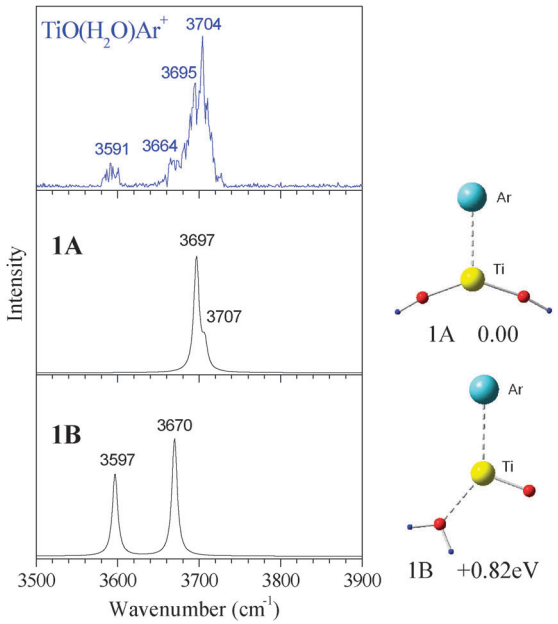

Fig. 2 IRPD spectrum of the $TiO(H_2O)Ar^+$ cluster and the simulated theoretical IR spectra of its low-lying isomers. The theoretical IR spectra were produced by using Lorentzian components with a full width at half-maximum of 10 cm^{-1}.

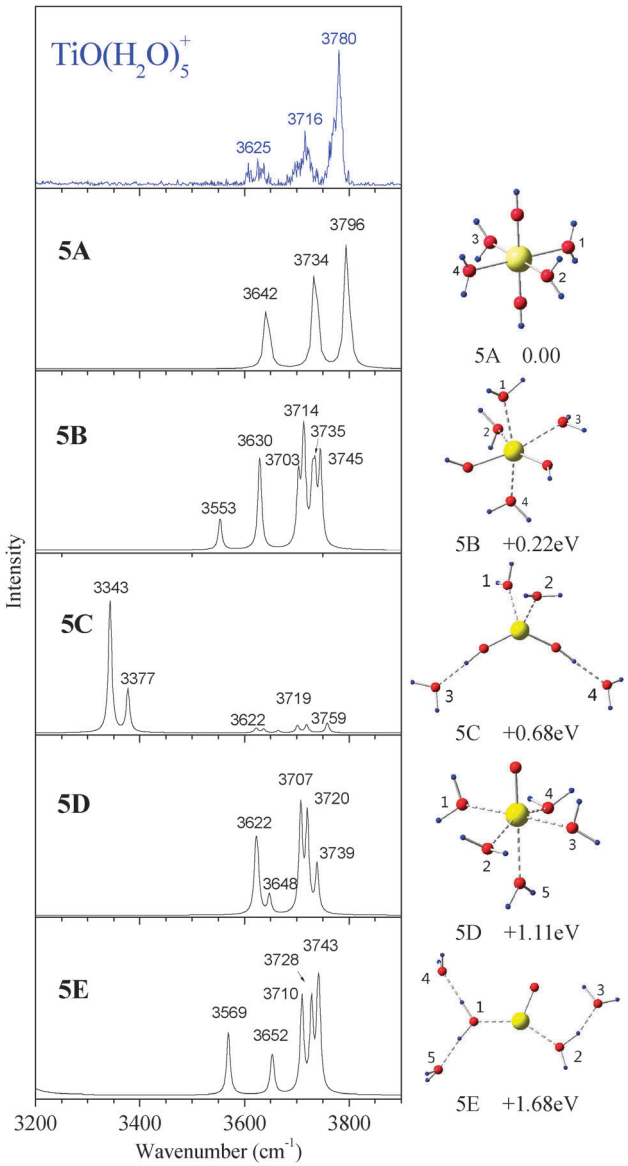

Fig. 3 IRPD spectrum of the $TiO(H_2O)_5^+$ cluster and the simulated theoretical IR spectra of its low-lying isomers. The theoretical IR spectra were produced by using Lorentzian components with a full width at half-maximum of 10 cm^{-1}.

$TiO(H_2O)_n^+$ (n = 5–7) clusters were obtained by monitoring the loss of a H_2O molecule as a function of the wavenumber of the infrared laser. The relative energies and the scaled theoretical vibrational frequencies of the low-lying isomers of $TiO(H_2O)Ar^+$ and $TiO(H_2O)_n^+$ (n = 5–7) clusters are summarized and compared with the experimental values in Table 1. The Cartesian coordinates of these low-lying isomers can be found in the ESI.† We would like to point out that it is difficult to predict the relative intensities of the peaks in the IRPD spectra precisely by theory because the interactions of clusters with photons in the experiments involve multiphoton processes, vibrational energy redistributions, and dissociations. Therefore, we mainly compare the theoretical and experimental band positions in this work.

$TiO(H_2O)Ar^+$

As seen in Fig. 2, the experimental IRPD spectrum of $TiO(H_2O)Ar^+$ exhibits two barely resolved strong peaks centered at 3695 cm^{-1} and 3704 cm^{-1}, a small shoulder at 3664 cm^{-1}, and a weak feature at 3591 cm^{-1}. The intensities of the 3695 and 3704 cm^{-1} peaks are much stronger than the 3664 and 3591 cm^{-1} peaks.

Theoretical calculations were performed to simulate the IRPD spectrum of $TiO(H_2O)Ar^+$. Before we conducted theoretical calculations on $TiO(H_2O)Ar^+$, we first calculated the structure of $TiO(H_2O)^+$ without the Ar atom. Our calculations indicated that there are two isomers for $TiO(H_2O)^+$, the first one (isomer A) is a C_{2v} planar dihydroxide structure ($Ti(OH)_2^+$) with two OH groups bonding to Ti^+ ions with an O–Ti–O angle of 139°, the second one (isomer B) is a C_s planar structure formed by TiO^+ and an intact H_2O molecule in which the O atom of the H_2O molecule interacts with the Ti end of the TiO^+ *via* an O–Ti–O angle of 111°. The energy of isomer B is higher than isomer A by 0.86 eV. The structure of isomer B is similar to the structure of $TiO(H_2O)^+$ reported by Deng *et al.*[31] although they found an O–Ti–O angle of 108°.

Our further calculations on the $TiO(H_2O)Ar^+$ cluster found two isomers (1A and 1B) corresponding to isomers A and B of $TiO(H_2O)^+$. They are formed by simply attaching an Ar atom to the Ti atom of isomers A and B. Isomer 1A is a C_s dihydroxide structure, with two OH groups bonding to the Ti atom. Isomer 1B has a H_2O molecule weakly interacting with TiO^+ through the oxygen atom of the H_2O. Isomer 1B is less stable than 1A by 0.82 eV. For isomer 1A, the frequency of H–OTiO–H asymmetric stretching is calculated to be ~3697 cm^{-1} and that of H–OTiO–H symmetric stretching is ~3707 cm^{-1}. These values are very

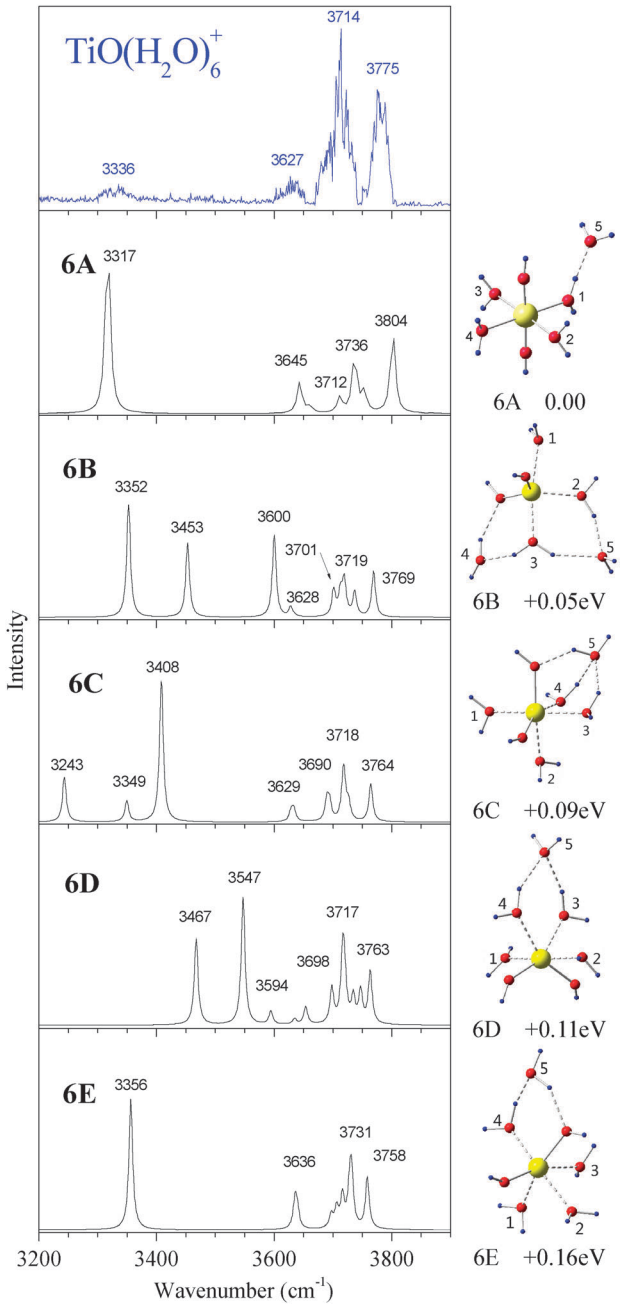

Fig. 4 IRPD spectrum of the $TiO(H_2O)_6^+$ cluster and the simulated theoretical IR spectra of its low-lying isomers. The theoretical IR spectra were produced by using Lorentzian components with a full width at half-maximum of 10 cm^{-1}.

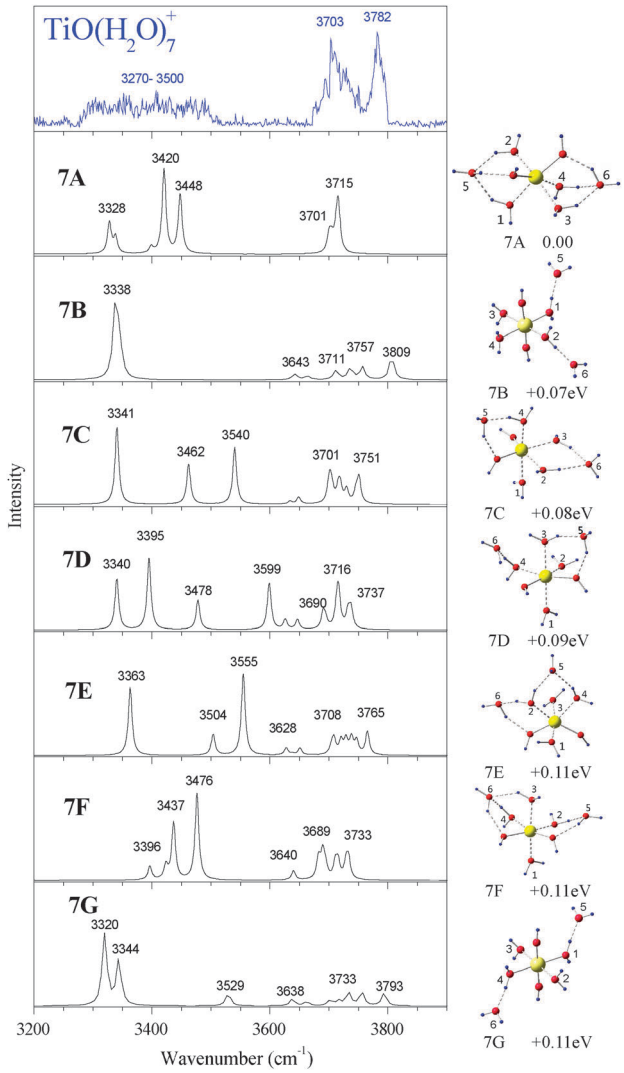

Fig. 5 IRPD spectrum of the $TiO(H_2O)_7^+$ cluster and the simulated theoretical IR spectra of its low-lying isomers. The theoretical IR spectra were produced by using Lorentzian components with a full width at half-maximum of 10 cm^{-1}.

close to the high frequency peaks at 3695 cm^{-1} and 3704 cm^{-1} in the experimental IRPD spectrum. It is worth mentioning that the Ar atom causes slight blue shifts in the vibrational frequencies of $Ti(OH)_2^+$ as the asymmetric and symmetric stretchings of H–OTiO–H in free $Ti(OH)_2^+$ are calculated to be 3684 and 3696 cm^{-1}, respectively, while those of $Ti(OH)_2Ar^+$ are 3697 and 3707 cm^{-1}. For isomer 1B, the frequency of H–O–H symmetric stretching is calculated to be 3597 cm^{-1} and that of H–O–H antisymmetric stretching is about 3670 cm^{-1}, they are red shifted compared to those of free H_2O (3657 and 3756 cm^{-1}). The vibrational frequencies of isomer 1B are consistent with the low-intensity peaks at 3591 and 3664 cm^{-1} in the IRPD spectrum of $TiO(H_2O)Ar^+$. The comparison of the theoretical calculations and the experimental IRPD spectrum confirmed that both isomers 1A and 1B exist in our experiments. It is quite surprising for isomer 1B to be detected in the experiments because isomer 1B is much less stable than isomer 1A. The existence of isomer 1B probably implies that there is a large energy barrier between isomer 1B and isomer 1A.

$TiO(H_2O)_5^+$

The experimental IRPD spectrum of $TiO(H_2O)_5^+$ exhibits three bands centered at 3625, 3716, and 3780 cm^{-1}, respectively. The band centered at 3780 cm^{-1} has higher frequency than the band (3704 cm^{-1}) in the spectrum of $TiO(H_2O)Ar^+$.

Fig. 3 shows five low-lying isomers of the $TiO(H_2O)_5^+$ cluster obtained by density functional calculations. Isomer 5A has an octahedral structure with two OH groups occupying the *para*

Table 1 Relative energies and vibrational frequencies of the low-lying isomers of $TiO(H_2O)^+$, $TiO(H_2O)Ar^+$, and $TiO(H_2O)_n^+$ (n = 5–7) clusters calculated at the B3LYP/6-311+G(d, p) level as well as the comparison with the experimental values

Cluster	Isomer	ΔE (eV)	Structure	Theoretical freq.[a] (cm^{-1})	Experimental freq. (cm^{-1})
$TiO(H_2O)^+$	A	0.00	C_{2v}	3684, 3696	
	B	0.86	C_s	3592, 3663	
$TiO(H_2O)Ar^+$	1A	0.00	C_s	3697, 3707	3695, 3704
	1B	0.82	C_1	3597, 3670	3591, 3664
$TiO(H_2O)_5^+$	5A	0.00	C_1	3642, 3643, 3646, 3734, 3735, 3796, 3799	3600–3650
	5B	0.22	C_2	3553, 3628, 3629, 3630, 3703, 3712, 3714, 3730, 3735, 3745	3680–3740
	5C	0.68	C_s	3343, 3377, 3622, 3637, 3665, 3665, 3702, 3719, 3758, 3759	3750–3800
	5D	1.11	C_2	3621, 3622, 3625, 3626, 3648, 3707, 3708, 3720, 3739	
	5E	1.68	C_1	3044, 3158, 3569, 3652, 3655, 3710, 3728, 3740, 3743	
$TiO(H_2O)_6^+$	6A	0.00	C_1	3317, 3642, 3643, 3645, 3661, 3712, 3736, 3753, 3802, 3804	3300–3350
	6B	0.05	C_1	3016, 3352, 3453, 3600, 3628, 3634, 3701, 3713, 3717, 3719, 3737, 3769	3600–3650
	6C	0.09	C_1	3243, 3349, 3408, 3629, 3633, 3690, 3694, 3717, 3718, 3719, 3727, 3764	3670–3740
	6D	0.11	C_1	3467, 3547, 3594, 3635, 3654, 3698, 3716, 3717, 3720, 3735, 3747, 3763	3750–3800
	6E	0.16	C_1	3356, 3635, 3636, 3640, 3697, 3706, 3716, 3728, 3731, 3732, 3758	
$TiO(H_2O)_7^+$	7A(7A)	0.00	C_1	3165, 3328, 3338, 3399, 3420, 3448, 3699, 3701, 3705, 3712, 3715, 3716, 3718	3270–3500
	7B	0.07	C_1	3338, 3345, 3641, 3643, 3663, 3711, 3713, 3735, 3737, 3756, 3757, 3806, 3809	3670–3750
	7C(7B)	0.08	C_1	3341, 3462, 3540, 3634, 3649, 3699, 3701, 3705, 3716, 3719, 3730, 3746, 3751	3750–3800
	7D(7C)	0.09	C_1	3032, 3340, 3395, 3478, 3599, 3626, 3647, 3690, 3694, 3714, 3715, 3717, 3732, 3737	
	7E(7D)	0.11	C_1	3102, 3363, 3504, 3555, 3628, 3638, 3651, 3704, 3708, 3720, 3729, 3738, 3747, 3765	
	7F(7E)	0.11	C_1	3047, 3396, 3424, 3437, 3476, 3640, 3682, 3689, 3691, 3695, 3711, 3715, 3729, 3733	
	7G	0.11	C_1	3320, 3344, 3529, 3638, 3662, 3702, 3717, 3733, 3755, 3756, 3793	

[a] A scaling factor of 0.96 is used.

sites and four water molecules in the same plane interacting with the Ti atom directly through their O atoms. Similar to isomer 5A, isomer 5B has a distorted octahedral structure with two OH groups at the *ortho* positions and four water molecules interacting with the Ti atom directly through their O atoms. Isomer 5B is less stable than isomer 5A by 0.22 eV. Isomer 5C has two water molecules attached to $Ti(OH)_2^+$ with their O atoms interacting with the Ti atom directly, it then has two additional water molecules interacting with the two OH groups of $Ti(OH)_2^+$ *via* hydrogen bonds. Isomer 5D is formed by attaching five water molecules to TiO^+ with their O atoms interacting with the Ti atom directly. Isomer 5E has two water molecules interacting with TiO^+ directly, then has three additional water molecules interacting with inner shell water molecules through hydrogen bonds. Isomers 5C, 5D, and 5E are less stable than isomer 5A by 0.68, 1.11, and 1.68 eV, respectively. Isomers 5A, 5B, and 5D have all water molecules in the inner shell. Isomer 5C has two H_2O molecules in the second solvent shell. Isomer 5E has three H_2O molecules in the second solvent shell.

In the simulated IR spectrum of isomer 5A, the peaks at 3642 and 3734 cm^{-1} are due to symmetric and anti-symmetric stretchings of H_2O(1, 2, 3, 4), respectively, these peaks are red shifted compared to those of free H_2O. The peak at 3796 cm^{-1} is due to the O–H stretching of $Ti(OH)_2^+$. It is blue shifted compared to the O–H stretchings of free $Ti(OH)_2^+$. The simulated IR spectrum of isomer 5A fits very well with the experimental IRPD spectrum of $TiO(H_2O)_5^+$. The peaks of isomer 5B at 3735 and 3745 cm^{-1} correspond to the O–H stretchings of $Ti(OH)_2^+$, which are also blue shifted compared to the O–H stretchings of free $Ti(OH)_2^+$. The peaks at 3703 and 3714 cm^{-1} are due to the anti-symmetric stretching of the H_2O molecules coordinated to the Ti atom of $Ti(OH)_2^+$. The peaks near 3553 and 3630 cm^{-1} are due to the symmetric stretchings of the H_2O molecules coordinating to the Ti atom of $Ti(OH)_2^+$. The peak at 3553 cm^{-1} is not observed in the experimental IRPD spectrum. In isomer 5C, the O–H stretchings of $Ti(OH)_2^+$ are red shifted to 3343 and 3377 cm^{-1} due to the formation of hydrogen bonds between $Ti(OH)_2^+$ and H_2O(3) as well as H_2O(4). These peaks are not observed in the experimental IRPD spectrum. The vibrational peaks of isomer 5D at 3622 cm^{-1} correspond to the symmetric stretchings of H_2O(1–4) surrounding the TiO^+ ion, that at 3648 cm^{-1} corresponds to the symmetric stretching of H_2O(5) connecting to Ti–O through the bottom, those at 3707 and 3720 cm^{-1} are due to the antisymmetric stretchings of H_2O(1–4), that at 3739 cm^{-1} is due to the asymmetric stretching of H_2O(5). These peaks are all red shifted compared to those of free H_2O. In isomer 5E, the O–H stretching of H_2O(1) is red shifted to 3158 cm^{-1} due to its interactions with the Ti atom and its neighboring H_2O molecules. The simulated IR spectra of isomers 5B, 5C, 5D, and 5E do not match the experimental spectrum very well. Also, they are much less stable than isomer 5A. Thus, the existence of isomers 5B, 5C, 5D, and 5E in the experiments can be ruled out. Isomer 5A is the most probable one detected in the experiments.

$TiO(H_2O)_6^+$

The experimental IRPD spectrum of $TiO(H_2O)_6^+$ has two strong bands centered at 3775 and 3714 cm^{-1} and two weak bands centered at 3627 and 3336 cm^{-1}, respectively. The band at

3714 cm^{-1} is much stronger than the similar band of $TiO(H_2O)_5^+$ observed at 3716 cm^{-1}. The band at 3336 cm^{-1} has not been observed in either the spectrum of $TiO(H_2O)Ar^+$ or that of $TiO(H_2O)_5^+$.

Our calculations show that the first five low-lying isomers of $TiO(H_2O)_6^+$ are very close in energy, differing by only 0.16 eV (Fig. 4). Isomer 6A can be considered to be derived from isomer 5A with the last water molecule added to the second shell interacting with the inner water molecule *via* a hydrogen bond. Isomer 6B has three water molecules in the inner shell interacting with the Ti atom of $Ti(OH)_2^+$ through their O atoms, then with the two additional water molecules in the second shell interacting with the two inner water molecules and one of the OH groups *via* hydrogen bonds. Isomer 6C has four inner water molecules interacting directly with the Ti atom of $Ti(OH)_2^+$ *via* their O atoms and an additional water molecule in the second shell. The structures of isomers 6D and 6E are generally similar to that of isomer 6C, all have one water molecule in the second shell interacting with the inner shell water molecules at different positions.

The simulated IR spectrum of isomer 6A shows a peak at 3804 cm^{-1} due to the O–H stretchings of $Ti(OH)_2^+$ and some peaks near 3645 and 3736 cm^{-1} corresponding to the symmetric and anti-symmetric stretchings of H_2O(2, 3, 4) respectively. In addition, isomer 6A also has a vibrational peak at $\sim$3317 cm^{-1}, which is due to the interaction of H_2O(1) with H_2O(5). The simulated IR spectrum of isomer 6A is in good agreement with the experimental IRPD spectrum of $TiO(H_2O)_6^+$. The theoretical calculations show that isomer 6B has a peak at 3453 cm^{-1} due to interaction of H_2O(4) with H_2O(3) and $Ti(OH)_2^+$, isomer 6C has peaks at 3243 and 3408 cm^{-1} due to the interactions among H_2O(5), H_2O(4), H_2O(3), and $Ti(OH)_2^+$, isomer 6D has peaks at 3467 and 3547 cm^{-1} due to the interactions among H_2O(3), H_2O(4), and H_2O(5). These peaks are not observed in the experimental IRPD spectrum. Thus, the existence of isomers 6B, 6C, and 6D in the experiments can be ruled out. The theoretical calculations found that isomer 6E has vibrational peaks near 3636 cm^{-1} due to the symmetric stretchings of H_2O(1), (2), and (3) at $\sim$3706 cm^{-1} due to the O–H stretching of H_2O(4), in the range of 3716 and 3731 cm^{-1} due to the anti-symmetric stretchings of H_2O(1), (2), (3), and (5), and at about 3758 cm^{-1} due to the free O–H stretching of $Ti(OH)_2^+$. Isomer 6E also has a vibrational peak at $\sim$3356 cm^{-1}, which belongs to the O–H stretching of H_2O(5) coordinating to the OH group of $Ti(OH)_2^+$. The simulated IR spectrum of isomer 6E is also consistent with the experimental IRPD spectrum. However, isomer 6E is less stable than isomer 6A by 0.16 eV. Therefore, we suggest isomer 6A to be the major one detected in the experiments. It is worth mentioning that, in the experimental IRPD spectrum of $TiO(H_2O)_6^+$, the peak at $\sim$3336 cm^{-1} has not been detected in the IRPD spectrum of $TiO(H_2O)Ar^+$ or that of $TiO(H_2O)_5^+$. The observation of this peak indicates that the sixth water molecule is added into the cluster in a different way compared to the other water molecules in $TiO(H_2O)Ar^+$ and $TiO(H_2O)_5^+$, that is the additional water molecule no longer coordinates directly with the Ti^+ ion, but starts to form hydrogen bonds with the OH groups of $Ti(OH)_2^+$ or the other H_2O molecules.

$TiO(H_2O)_7^+$

The experimental IRPD spectrum of $TiO(H_2O)_7^+$ cluster contains two strong features centered at 3782 and 3703 cm^{-1} and a very broad feature in the range of 3270–3500 cm^{-1}.

As seen in Fig. 5, the first seven isomers of $TiO(H_2O)_7^+$, isomers 7A–7G, are very close in energy with isomer 7G higher than isomer 7A by only 0.11 eV. They all have four inner water molecules interacting directly with the Ti atom of $Ti(OH)_2^+$ *via* their O atoms and two additional water molecules in the second shell. Isomers 7A, 7C, 7D, and 7E can be considered to be derived from isomer 5B by adding two additional water molecules to the second shell, while isomers 7B and 7G can be derived from isomer 5A by attaching two water molecules in the second shell. All of these isomers have an inner core similar to isomers 5A and 5B, composed of $Ti(OH)_2^+$ and four water molecules. The only differences among them are the positions of the two H_2O molecules in the second shell.

The theoretical calculations show that the stretching modes of the water molecules are red shifted due to the formation of hydrogen bonds among the water molecules and $Ti(OH)_2^+$, thus, isomer 7A has vibrational peaks at 3328, 3338, 3399, 3420, and 3448 cm^{-1}, which fall into the region of the very broad feature between 3270 and 3500 cm^{-1} in the experimental IRPD spectrum of $TiO(H_2O)_7^+$. Isomer 7A also has vibrational peaks at 3701 and 3715 cm^{-1} which are red shifted relative to the antisymmetric stretching of free H_2O molecules, in agreement with the 3703 cm^{-1} feature in the experimental spectrum. The theoretical calculations show that isomer 7B has vibrational peaks at 3338 cm^{-1} due to the O–H stretching of H_2O(1) and H_2O(2) connecting to H_2O(5) and H_2O(6) molecules in the second shell, at 3643 and 3757 cm^{-1} due to symmetric and anti-symmetric stretchings of H_2O(3, 4, 5, 6), respectively, and at 3809 cm^{-1} due to the O–H stretchings of $Ti(OH)_2^+$. The simulated IR spectrum of isomer 7B is also in agreement with the experimental IRPD spectrum of $TiO(H_2O)_7^+$. Therefore, isomers 7A and 7B more likely coexist in our experiments. Isomers 7C, 7D, and 7E have many IR peaks in the range of 3270–3500 cm^{-1} as well. The theoretical calculations show that isomers 7C, 7D, 7E, and 7G have peaks at 3540, 3599, 3555, and 3529 cm^{-1}, respectively. These peaks have not been detected in the experimental IRPD spectrum of $TiO(H_2O)_7^+$. In addition, the peaks of isomers 7F and 7G at 3640 and 3638 cm^{-1} are much different from the experimental peaks near 3703 cm^{-1}. Thus, the existence of isomers 7C, 7D, 7E, 7F, and 7G in our experiments can be ruled out.

Our studies show that $Ti(OH)_2^+$ and (H_2O)–TiO^+ types of products can be formed when TiO^+ interacts with the first water molecule. $Ti(OH)_2^+$ is much more stable than (H_2O)–TiO^+. This finding is different from previous results reported by Deng *et al.*,[31] in which only the less stable (H_2O)–TiO^+ type of product was considered. The $Ti(OH)_2^+$ type of structure becomes more dominant when TiO^+ interacts with more water molecules. The structure of $TiO(H_2O)_5^+$ can be written as $[Ti(OH)_2](H_2O)_4^+$,

which is characterized by attaching four water molecules to a $Ti(OH)_2^+$ core with their O atoms coordinating directly with the Ti atom. In this structure, the two OH groups and four water molecules form a complete shell around the Ti atom, therefore, make the cluster more stable. When the number of water molecules increases further, the additional water molecules are added to the second shell. This is consistent with the predominant mass peak of $TiO(H_2O)_5^+$ observed in the mass spectrum of $TiO(H_2O)_n^+$ clusters (Fig. 1) and the decrease of the mass intensities of $TiO(H_2O)_6^+$ and $TiO(H_2O)_7^+$ compared to that of $TiO(H_2O)_5^+$.

IV. Conclusions

We investigated $TiO(H_2O)Ar^+$ and $TiO(H_2O)_{5-7}^+$ clusters with infrared photodissociation (IRPD) spectroscopy and density functional theory calculations. The observation of the high frequency bands at 3695 and 3704 cm^{-1} and low frequency bands at 3664 and 3591 cm^{-1} in the IRPD spectrum of $TiO(H_2O)Ar^+$ confirmed the existence of two isomers in the forms of $Ti(OH)_2Ar^+$ and (H_2O)–$TiOAr^+$, respectively, with the first isomer being dominant. In the structure of $TiO(H_2O)_5^+$, four water molecules are attached to a $Ti(OH)_2^+$ core with their O atoms coordinating directly with the Ti atom. In $TiO(H_2O)_6^+$ and $TiO(H_2O)_7^+$ clusters, the sixth and seventh water molecules were added to the second solvent-shell. The emergence of the 3336 cm^{-1} band for $TiO(H_2O)_6^+$ and the 3270–3500 cm^{-1} band for $TiO(H_2O)_7^+$ indicates that the sixth and seventh water molecules form hydrogen bonds with the inner shell water molecules or the OH groups of $Ti(OH)_2^+$ rather than coordinating directly with the Ti atom. In $TiO(H_2O)_n^+$ clusters with $n \geq 5$, the coordination number of the Ti atom is six, including two OH groups and four water molecules.

Acknowledgements

This work was supported by the Natural Science Foundation of China (Grant No. 20933008) and the China Postdoctoral Science Foundation (No. 2012T50138). The theoretical calculations were conducted on the ScGrid and Deepcomp7000 of the Supercomputing Center, Computer Network Information Center of Chinese Academy of Sciences.

References

1 B. Meunier and W. Adam, *Metal-oxo and metal-peroxo species in catalytic oxidations*, Springer, Berlin, New York, 2000, structure and bonding, 97.
2 Y. Zhang, Y. Chen, P. Westerhoff, K. Hristovski and J. C. Crittenden, *Water Res.*, 2008, **42**, 2204.
3 V. M. Aroutiounian, V. M. Arakelyan and G. E. Shahnazaryan, *Sol. Energy*, 2005, **78**, 581.
4 Y. Gong, M. Zhou and L. Andrews, *Chem. Rev.*, 2009, **109**, 6765.
5 G. E. Brown, V. E. Henrich and W. H. Casey, *et al.*, *Chem. Rev.*, 1999, **99**, 77.
6 J. R. T. Johnson and I. Panas, *Inorg. Chem.*, 2000, **39**, 3181.
7 J. R. T. Johnson and I. Panas, *Inorg. Chem.*, 2000, **39**, 3192.
8 G. K. Koyanagi, D. K. Bohme, I. Kretzschmar, D. Schroder and H. Schwarz, *J. Phys. Chem. A*, 2001, **105**, 4259.
9 S. Feyel, D. Schroder and H. Schwarz, *Eur. J. Inorg. Chem.*, 2008, 4961.
10 S. Barsch, D. Schroder and H. Schwarz, *Chem.–Eur. J.*, 2000, **6**, 1789.
11 J.-B. Ma, Y.-X. Zhao, S.-G. He and X.-L. Ding, *J. Phys. Chem. A*, 2012, **116**, 2049.
12 X. N. Li, B. Xu, X. L. Ding and S. G. He, *Dalton Trans.*, 2012, **41**, 5562.
13 D. W. Rothgeb, E. Hossain, A. T. Kuo, J. L. Troyer, C. C. Jarrold, N. J. Mayhall and K. Raghavachari, *J. Chem. Phys.*, 2009, **130**, 124314.
14 D. W. Rothgeb, E. Hossain, N. J. Mayhall, K. Raghavachari and C. C. Jarrold, *J. Chem. Phys.*, 2009, **131**, 144306.
15 N. J. Mayhall, D. W. Rothgeb, E. Hossain, C. C. Jarrold and K. Raghavachari, *J. Chem. Phys.*, 2009, **131**, 144302.
16 D. W. Rothgeb, J. E. Mann and C. C. Jarrold, *J. Chem. Phys.*, 2010, **133**, 054305.
17 Y. Gong and M. F. Zhou, *ChemPhysChem*, 2010, **11**, 1888.
18 M. F. Zhou, J. Zhuang, G. J. Wang and M. H. Chen, *J. Phys. Chem. A*, 2011, **115**, 2238.
19 R.-Z. Li, H.-G. Xu, G.-J. Cao, Y.-C. Zhao and W.-J. Zheng, *J. Chem. Phys.*, 2011, **135**, 134307.
20 H. M. Dyck and E. N. Tyler, *Astron. J.*, 2002, **124**, 541.
21 Z. G. Shang, Z. Q. Liu, P. J. Shang and J. K. Shang, *J. Mater. Sci. Technol.*, 2012, **28**, 385.
22 A. Fujishima and K. Honda, *Nature*, 1972, **238**, 37.
23 E. Martinez-Ferrero, Y. Sakatani, C. Boissiere, D. Grosso, A. Fuertes, J. Fraxedas and C. Sanchez, *Adv. Funct. Mater.*, 2007, **17**, 3348.
24 T. Tachikawa, M. Fujitsuka and T. Majima, *J. Phys. Chem. C*, 2007, **111**, 5259.
25 X. B. Chen, L. Liu, P. Y. Yu and S. S. Mao, *Science*, 2011, **331**, 746.
26 T. L. Thompson and J. T. Yates, *Chem. Rev.*, 2006, **106**, 4428.
27 A. Kudo and Y. Miseki, *Chem. Soc. Rev.*, 2009, **38**, 253.
28 X. F. Wang and L. Andrews, *J. Phys. Chem. A*, 2005, **109**, 10689.
29 M. Q. Fatmi, T. S. Hofer, B. R. Randolf and B. M. Rode, *J. Comput. Chem.*, 2007, **28**, 1704.
30 J. Blazevska-Gilev, V. Jandováa, J. Kupčíka, Z. Bastl, J. Šubrtd, P. Bezdičkad and J. Pola, *J. Solid State Chem.*, 2013, **197**, 337.
31 H. Deng, K. P. Kerns, B. C. Guo, R. C. Bell and A. W. Castleman, *Croat. Chem. Acta*, 1998, **71**, 1105.
32 D. Schröder, J. Roithová and H. Schwarz, *Int. J. Mass Spectrom.*, 2006, **254**, 197.
33 D. Schröder and H. Schwarz, *Int. J. Mass Spectrom.*, 2003, **227**, 121.
34 D. Vukomanovic and J. A. Stone, *Int. J. Mass Spectrom.*, 2000, **202**, 251.
35 D. Schröder, *J. Phys. Chem. A*, 2008, **112**, 13215.

36 D. Schröder, S. O. Souvi and E. Alikhani, *Chem. Phys. Lett.*, 2009, **470**, 162.
37 S. W. Sigsworth and A. W. Castleman, *J. Am. Chem. Soc.*, 1992, **114**, 10471.
38 J. R. Sambrano, L. Gracia, J. Andrés, S. Berski and A. Beltrán, *J. Phys. Chem. A*, 2004, **108**, 10850.
39 J. R. Sambrano, J. Andrés, L. Gracia, V. S. Safont and A. Beltrán, *Chem. Phys. Lett.*, 2004, **384**, 56.
40 A. Ricca and C. W. Bauschlicher, Jr., *J. Phys. Chem. A*, 1997, **101**, 8949.
41 J. M. Lisy, *J. Chem. Phys.*, 2006, **125**, 132302.
42 M. A. Duncan, *Int. Rev. Phys. Chem.*, 2003, **22**, 407.
43 Y. C. Zhao, Z. G. Zhang, J. Y. Yuan, H. G. Xu and W. J. Zheng, *Chin. J. Chem. Phys.*, 2009, **22**, 655.
44 C. T. Lee, W. T. Yang and R. G. Parr, *Phys. Rev. B: Condens. Matter Mater. Phys.*, 1988, **37**, 785.
45 A. D. Becke, *J. Chem. Phys.*, 1993, **98**, 1372.
46 G. W. T. M. J. Frisch and H. B. Schlegel, *et al.*, GAUSSIAN 09, Revision A.02, Gaussian, Inc., Wallingford, CT, 2009.
47 M. W. Wong, *Chem. Phys. Lett.*, 1996, **256**, 391.